Time and Frequency Domain Assessment of Low-Power MEMS Accelerometers for Structural Health Monitoring

Time and Frequency Domain Assessment of Low-Power MEMS Accelerometers for Structural Health Monitoring

Emanuele Parisi, Amirhossein Moallemi, Francesco Barchi, Andrea Bartolini,
Davide Brunelli, Nicola Buratti, Andrea Acquaviva
Department of Electrical, Electronics and Information Engineering
University of Bologna
Bologna, Italy
emanuele.parisi@unibo.it

***Abstract*—Nowadays, MEMS sensors are widely used in several applications, including SHM. Although they do not outperform professional piezo accelerometers, because of their significantly lower cost and power consumption, they enable extensive, pervasive and battery-less monitoring systems. For these applications, it is critical to assess their performance in typical SHM signal processing tasks and in realistic monitoring scenarios. This paper presents an experimental performance evaluation of representative MEMS devices for SHM applications, providing a guideline and insightful results about the opportunities and capability of these devices in challenging scenarios for such COTS components. Results demonstrate that MEMS-based accelerometers are a feasible solution to replace expensive piezo-based accelerometers. Deploying digital MEMS in Low-Power mode is promising to minimise sensor node energy consumption with savings up to 80% in the best case. Time and frequency domain analysis shows that MEMS can detect modal frequencies, an important parameter for damage detection, with a maximum 1.6% error.**

***Index Terms*—SHM; MEMS accelerometers; Low-Power system.**

I. Introduction

Civil infrastructures degrade over time due to use, accidental events, or harsh environmental conditions. Considering the constant growth of large-scale civil infrastructures built worldwide, a cost-effective solution for continuous observation of structural integrity is becoming an essential requirement for their maintenance [1]. Structural Health Monitoring (SHM) techniques assess the structural state and determine the required maintenance and repair. The core component for such a monitoring system is represented by accelerometers that have to acquire the vibration of the infrastructure to provide data for experts' analysis. Resolution is one of the most important performance requirements for such an application, and so far, high-accurate low-noise density piezoelectric-based sensors are widely recognized as the most accurate transducers for such operations [2]. In the last decades, MEMS (Micro-Electro-Mechanical Systems) capacitive accelerometers have also been introduced and experimented with such scenarios. Their extreme low-cost and low-power permits to design and deploy a steady measurement infrastructure for continuous monitoring, to scale up to hundreds of measurement points for a single building, which is unfeasible using piezo accelerometers, that are two orders of magnitude more expensive. Nevertheless, MEMS accelerometers do not outperform piezo accelerometers because commercial devices are designed to measure larger bandwidth signals and are characterized by lower sensitivity, thus requiring complex signal conditioning electronics to achieve acceptable noise floor [3]. For this reason, to unveil the potential of these devices, a comparison with piezo accelerometers and a characterization of representative MEMS device, currently missing in literature, is needed. This paper presents the characterization in both time and frequency domains of representative MEMS devices, focusing on SHM application-specific metrics and using either a laboratory set-up and a real infrastructure. Moreover, we investigate the metrological properties of digital MEMS that feature two working modes, namely Low-Power (LP) and High-Performance (HP), allowing to trade sensor power consumption for measurement accuracy. To this purpose, we realized a prototyping board, equipped with a pair of digital MEMS configured one in High-Performance and the other in Low-Power mode, thus simultaneously measuring the same stimuli. Comparisons are carried out using a piezoelectric accelerometer as a reference. This paper has two main contributions: i) We investigate measurement accuracy of analog and digital MEMS configured in High-Performance and Low-Power mode comparing with a seismic piezoelectrical accelerometers using both in-lab experiments and measurements taken on a real-world structure; ii) We provide an evaluation of the energy consumption of digital devices in Low-Power mode to highlight the advantages of using such configuration in place of High-Performance mode. To this purpose, we designed an energy model tailored to reference state-of-art nodes. The paper is organized as follows. Section II describes the related work. Section III introduces the sensors used in our analysis; Section IV describes our real structures used for experiments. The methodology of our analysis is discussed in Section V, whereas results and final discussion are in Section VI. Section VII concludes the paper.

II. Related Work

In recent year, the MEMS technology has become important for several applications, such as bioengineering, automation and structural health monitoring [4]. Since their introduction, the reliability and performance of such sensors compared to

the earlier, more expensive sensors have been a challenge to the community. Some works in the literature provided generic reviews comparing wireless MEMS-based accelerometers sensor boards for SHM [1], and Seismology [5]. Several evaluations characterized early analog MEMS performances with lab-based frames. For example, the work in [6] compared one analog MEMS-based with PCB accelerometers for modal analysis with three different excitations. Further, [7] delved more into analog MEMS by characterizing four different sensors in noise level, frequency, and sensitivity metrics. To avoid the relatively high noise level of the early MEMS accelerometer, the work in [8] designed two custom sensors for SHM applications with low bandwidth, thus resulting in a diminished noise level of MEMS.

More advanced analog and digital MEMS with deployability in embedded systems have been introduced to the community during the last decade, opening an ocean of options. To characterize these new MEMS, [2] evaluated two analog and four digital commercial MEMS sensors targeting frequency and damping identification for civil structures. By experimenting on a small concrete slab structure, they conclude that low-cost MEMS are feasible options to replace expensive piezoelectric ones. However, to conduct this conclusion, testing conditions differ for each sensor type, thus introducing heterogeneity in the dataset. Similarly, [9] computed displacement over a small scale reinforced concrete (RC) beam to detect cracks exploiting four different accelerometer sensors. Although MEMS performed better to detect early cracks in the beam, PZT detected the final failure of the structure. Small RC structures characterized sensors better than steel-frame; nevertheless, a real-life scenario case with a long, aged concrete highway where ambient noise plays a critical role is missing in the above-mentioned characterizations.

The work [3] provides the most reliable digital and analog sensors characterization by prototyping a self-made tri-axial accelerometer, i.e., Kionix KXR94-2050, and a referenced accelerometer PCB 356A16, to validate the applicability of MEMS practically over the cable-stayed bridge in Italy. Experimental Model Analysis (EMA) and Finite Element Analytical estimations (FEA) demonstrate that MEMS accelerometer can be a reliable substitute for expensive piezoelectric sensors. In a similar vein, we further investigate two scenarios (one real-case and one laboratory) targetting a variety of low-cost commercial MEMS accelerometers.

Compared to other works, we initially characterize analog and digital MEMS vs piezoelectric sensors in real-life case experiments. Furthermore, benefiting from recent digital MEMS's High-Performance and Low-Power features, we characterize these two modes both in the time and frequency domain.

III. Accelerometer Sensors

This section describes the three different sensors technologies chosen for the comparisons of this work, including a highly accurate expensive piezoelectric, PCB393B12, an ultra-compact linear low-cost analog MEMS, namely LIS344ALH, and a dual-mode always-on 3D digital MEMS, namely ISM330DHCX. Other than SHM, smart infrastructure and inertial navigation are fields of interest for such sensors.

1) PCB393B12: is a uni-axial Integrated Circuit Piezoelectric (ICP) accelerometer sensor benefiting from a low-cost coaxial cables connector to interface with the data logger. This sensor operates by applying a constant current signal. The ICP technology converts the high impedance acquired data to a low impedance output signal capable of unconditionally transmitting lines with long cables. Furthermore, the low-noise output voltage is compatible with data analysis methodologies.

2) LIS344ALH: is an ultra-compact three-axis linear accelerometer including a sensing element and an IC interface system. The sensing element is fabricated by the STMicroelectronics production line for sensors and actuators in silicon, and it is adept at detecting accelerations. Similarly, the IC interface is manufactured deploying the CMOS process with a high level of integration developed by ST. The major task of the IC interface is to convert the information acquired by the sensing element into an analog signal for the external world.

3) ISM330DHCX: is a system-in-package including a high-performance 3D digital accelerometer and 3D digital gyroscope tailored for Industry 4.0 applications. The manufacturing process for various sensing elements and IC interfaces is similar to the one described in Sec. III-2. Since it is a digital system, it introduces adjustability to the system. For instance, a set of programable computational features such as Machine Learning (ML) core, an accessible and programmable Finite State Machine (FSM), and 9 kB FIFO to store data temporarily and perform real-time analysis, provide the user with an intelligent sensor at low power. Furthermore, this accelerometer benefits from two modes, namely, high-performance and low-power, where these modes can be used to reduce the system's total energy consumption.

IV. Structural Health Monitoring Frameworks & Scenarios

A. SHM Frameworks

Fig. 1 illustrates the two systems used to acquire and store the data. Fig. 1-A presents the SHM node composed of an analog MEMS and two digital MEMS accelerometers (one for low-power configuration and the second one for high-performance configuration), a temperature sensor, a humidity sensor, a micro sd-card to store the data, a NB-IoT module to transmit data to the cloud, and a low power host microcontroller, STM32L476VGTx, to control the system. The sampling frequency of the analog accelerometer is 25.6 kHz, followed by a filtering and subsampling procedure resulting in a readout frequency of 100 Hz and resolution of 16 bits. The digital accelerometers configured in HP mode samples measurements at a frequency of 833 Hz and filters them using a on-board low-pass filter with a cut-off frequency of half the output data rate. The digital device in LP mode samples at a frequency of 52 Hz and filters measurements using a on-board low-pass filter with a constant cut-off frequency of 780 Hz. Both HP and LP modes produce 16-bits measurements. Figure 1-B provides the piezoelectric sensor acquisition network, where an ADC convertor translates the acquired analog signal to a store-able

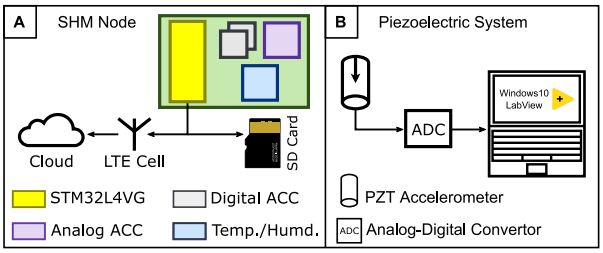

Fig. 1. The two Acquisition systems were deployed to evaluate the sensors. In panel A) MEMS-based setup configuration, B) Piezoelectric-based setup configuration

digital one. This sensor operates with a sampling frequency of 500 Hz.

B. Experiment Description

1) In-Lab Experiments: This experiment utilised a Material Test System (MTS) shaker to excite vertically the sensors described in Sec. III with sinusoidal stimuli. It was carried out to investigate the performance of measurements systems benefiting from commercial MEMS and piezoelectric accelerometer. Since structures operate under low frequency, we fixed the excitation frequency of the shaker at 10 Hz, while sweeping the amplitude range of the excitation from 30 to 250 μm. The intuition behind this experiment was to simulate various ranges of input excitation to estimate real-life random value inputs excitations in long-span bridges or structures. A plate is attached to the shaker, holding the mounted sensors. Screws fix the MEMS sensors, and the piezo one is attached to the bottom of the plate by a steel magnet connector.

2) Concrete Beam Experiment: To assess the performance of devices under test in a real-world scenario, we carried out a set of measurements on a concrete beam. The beam was composed of a concrete slab supported by two steel towers at each end. The total length of the beam is 25.9 m, while the width is 1.6 m. The monitoring system described in Sec. IV-A was mounted at the middle of the beam for the experiment duration. The experiment started by charging the beam with an even number of plates (1x1x0.25 m), each weight 1800 kg. After charging four plates over the beam, some additional wedge was added to the towers holding the beam to avoid rigid torsion rotation. The experiment aimed to charge and discharge the beam until cracks appeared.

V. Methodology

This section describes the methodology we use to assess MEMS accuracy and Low-Power mode energy efficiency. Subsection V-A describes time and frequency domain analysis to characterize MEMS metrological performance. Subsection V-B details the energy model we propose and the reference application and sensor node we tailor it to.

A. Metrological characterization methodology

The primary task of structural health monitoring is to collect building health information, unveiling potentially harming issues such as damages and ageing. In dynamic monitoring applications a set of sensors collect accelerometric data to feed modal identification algorithms and to perform early damage detection and structural health assessment analysis. We compare accelerometer performance in the frequency and time domain through the analysis of the measurements taken during the two experiments described in Subsection IV-B.

To evaluate measurement quality in the time-domain, we first set the relevant metrics for damage detection. Structural vibrations can be modeled as dampened oscillations depending on three parameters, namely frequency, amplitude and damping factor. As such, by fitting the sensor measurements with this model using the Ordinary Least Squares method, we evaluate the accuracy of the selected accelerometers in inferring these structural parameters. The model for the In-Lab experiments, described in Equation 1, is parametric with respect to signal amplitude (c_0), frequency (c_1) and phase (c_2).

$$f_{lab}(t) = c_0 sin(c_1 t + c_2) \tag{1}$$

Equation 2 approximates the dynamic behaviour of the beam as a single degree of freedom spring-mass-damper system. For this purpose, a further coefficient (c_3) is introduced to model the decay factor of structural oscillations in time.

$$f_{beam}(t) = c_0 e^{-c_3 t} sin(c_1 t + c_2) \tag{2}$$

Frequency-domain analysis focuses on assessing the quality of the power spectral density (PSD) that can be obtained when analysing the measurements of the different devices. Describing the accuracy of the PSD of a signal is of paramount importance since most frequency-domain modal identification and damage detection algorithms are built on top of PSD computation. For each experiment, we estimate the PSD of the measured signal using the Welch method, choose the most prominent peak and compute three metrics: (i) natural frequency, (ii) amplitude and (iii) width. Peak frequency is an important parameter to assess structural health and a number of state-of-the-art damage detection pipelines observe shifts in the natural frequencies of a structure to detect anomalies [10]. Peak amplitude and width are also relevant since they play a role in the estimation of modal shape and structural damping, two modal parameters that can be observed to detect changes in structural dynamic behaviour. According to the Half-Power method, peak width is estimated as the distance between the peak intercepts at amplitude $p/\sqrt{2}$, where p is the peak height. For in-lab experiment, the most prominent peak corresponds to the tone in the spectrum corresponding to the frequency of the sinusoidal input stimulus applied by the MTS machine. Instead, for beam measurements the most prominent peak represents the first modal frequency of the structure. To complete frequency domain analysis, we estimate device noise from a "silent" portion of the real-life experiments where no excitation was applied to the sensors. We estimate noise both in the frequency domain, computing the square root of the average of the noise PSD, and in the time domain, computing the root mean square (RMS) of the measured noise signal.

B. Digital MEMS energy model description

In the context of continous monitoring applications, the energy budget for a battery-less sensor node needs to be carefully evaluated. Recent digital MEMS devices can be driven two working modes: High-Performance and Low-Power. Low-Power mode reduces power consumption by duty cycling the

reading circuitry of the sensing element trading measurement precision for a lower power consumption. However, the impact of Low-Power mode on the energy consumed by the whole sensor node has not yet been investigated. Such verification is important to take into account MCU computation and data transmission in the energy cost evaluation.

We propose a energy model for a sensor nodes composed of a digital MEMS accelerometer, a processing MCU and a radio transceiver, inspired by the one presented in [4]. The MCU belongs to the STM32L4 series, a System-on-Chip (SoC) optimised for low-power edge computation. It saves energy during idleness driving the SoC to STOP state which minimises energy consumption while retaining memory. The sensor is the StMicroelectronics ISM330DHCX that communicates through SPI. While the node presented in [4] enables remote communication using the NB-IoT protocol, we consider Energy Per Bit (EPB) transmission energy a free parameter. This allows us to describe how Low-Power mode energy gain changes for different radio technologies. The monitoring application we model has the following workload: (a) The MEMS measures accelerations for t_a seconds at a rate of f_s Hz. The MCU wakes-up to read measurements as they are ready and then returns idle. (b) The MCU processes recorded accelerations to infer the structural health of the building being monitored. (c) The result of the processing pipeline is transferred to the radio. Among the many embedded protocols available we choose UART since it is widely adopted and available in many radio transceiver. (d) The radio sends the data to the cloud. Given components $C = \{mems, mcu, radio\}$ and workload stages $S = \{a, b, c, d\}$, system energy is modeled as:

$$E = \sum_{s}^{S} t_s \sum_{c}^{C} P_{c,s} \tag{3}$$

Time t_a depends on the number of samples taken and f_s, the sampling frequency of the sensor. Time t_b is a variable parameter to make our model independent on the actual processing performed by the MCU. Time t_c depends on the amount of data to be moved to the radio for transmission. $P_{mcu,a}$, the power consumed by the MCU during stage a, is the weighted average in run and stop mode since MCU continously switch on and off to read new measured acceleration value:

$$P_{mcu,a} = xP_{mcu,run} + (1-x)P_{mcu,stop} \tag{4}$$

$$x = \frac{Bf_s}{bps_{spi}} \tag{5}$$

where x is the fraction of time where the MCU is reading measurement samples. Here, bps_{spi} is the rate at which B bits are transferred over SPI, while f_s is the sampling frequency of the MEMS.

VI. Results

In this section, our main focus is on analyzing the evaluation of the two MEMS with the accurate piezoelectric accelerometer employing the three domains proposed in Sec. V. Utilizing a lab-scale shaker, we first evaluate the performance of each sensor by sinusoidal excitations with a small and large amplitudes. Then, we study the results achieved in the in-lab experiments with a real-life scenario on a concrete beam.

TABLE I
Estimation of Noise in the time and frequency domain

	PCB	LIS	ISM_H	ISM_L
$\mu g/\sqrt{Hz}$	10.28	23.98	65.86	436.20
mg_{RMS}	0.06	0.12	0.35	2.19

TABLE II
In-time Analysis for the Lab and Beam experiments.

Experiment		Signal Frequency [Hz]				Signal Amplitude [mg]			
		PCB	LIS	ISM_H	ISM_L	PCB	LIS	ISM_H	ISM_L
LAB	$30\,\mu m$	10.0	10.0	10.0	9.9	10	9	10	24
	$250\,\mu m$	10.0	10.0	10.0	9.9	91	86	100	120
Experiment		Signal Frequency [Hz]				Decay Factor [1e-3]			
BEAM		5.50	5.54	5.59	5.57	8.3	8.6	8.3	11.6

Finally, we provide an energy modelling system deploying MEMS jointly with various communication protocols and a low-power processing unit.

A. Noise Analysis

Ambient noise is a consistently, non-zero element present in acquisition systems. Having a low noise level is an essential key in designing analog and digital devices such as a sensor to avoid the inference of small valuable signals and noise.

Since the advanced processing methodologies that assess a structure's condition deploy both the time and frequency domain, we performed noise analysis in the time and frequency domain. Tab. I indicates that the piezoelectric sensor, PCB393B12, benefits from the lowest noise level with only $0.06\,mg_{\text{RMS}}$ and $10.28\,\mu g/\sqrt{Hz}$ for the time and frequency domain, respectively. The second best place is analog MEMS, where the noise level is approximately double than the PCB sensor. On the contrary, the noise level of the digital MEMS accelerometer increases drastically where Tab. I reports that ISM in low-power suffers from $2.2\,mg_{\text{RMS}}$ to $436.2\,\mu g/\sqrt{Hz}$, i.e. one order of magnitude higher than the piezoelectric sensor in both time and frequency domain. The former difference is due to the low power consumption of the digital sensors, since there is a trade-off betweeen noise level and power consumption. To conclude, the results in Tab. I show that the costly piezo sensor benefits from a low noise level; thus, it could be the best choice for monitoring systems with no constraint on power consumption. However, analog MEMS can provide a similar noise level for dense scalable monitoring systems with constraints on budget and power.

B. Time Analysis

Recent studies have demonstrated the feasibility of deploying raw time-series signals as input features to monitor large-scale structures, especially damage detection methodologies. Therefore, we fit a model based on the formulation described in Sec.V. For the in-lab experiments, we fit the acquired data of a sinusoidal impulse where the two critical parameters are signal amplitude and frequency. Next, we study signals frequency and decaying exponential factor for the real-life experiment. Tab. II reports the result of the fitted models for the former parameters.

For the in-lab experiment, the small amplitude stimuli, i.e. $30\,\mu g$, Tab.II reports that it is harder for digital MEMS in LP

mode to fit the exact amplitude of the stimuli compared to the piezo one. However, the digital sensor in HP mimics the piezo by zero error. ISM in low-power mode deviates from the nominal value because the signal with a small amplitude is equal to the noise level; hence the fitting algorithm is not capable to find the optimum solution for the data. By increasing the nominal value to 250 μg, ISM in low-power mode error is less than 30 %, while for the other two cases, the error diminishes to less than 10% compared to the piezo one, indicating that MEMS operates better with larger signals than smaller ones. Furthermore, all the sensors can perfectly fit the signal's frequency with a slight error for the ISM in LP mode compared to the nominal value. For the real-life experiment, we consider the value obtained by the piezo as the most accurate one, with a 5.5 Hz signal frequency and 8.3 m decaying factor. The bottom part of Tab. II reports that ISM in HP and LIS can mimic the behaviour of the piezo with the same decaying factor, whereas the ISM in LP decays faster by 41.20%. Next, the signal frequency section of Tab. II reports that LIS has the closest estimation to the piezo with only 0.04 Hz difference, while ISM has a similar error with 0.09 Hz and 0.07 Hz for HP and LP modes compared to the piezo sensor, respectively. In conclusion, MEMS-based sensors imitate the piezo manners in acquiring frequency and amplitude signals in the time domain. However, the ISM in low-power decays faster than the other two sensors due to low sampling rate and high noise level.

C. Frequency Analysis

Frequency Analysis is one of the primary methods used by civil engineers to monitor structures' modification and identify damages by deploying metrics like peak frequency, amplitude, and width. We utilize the PSD method described in Section V to extract former frequency parameters. For the in-lab experiment, we translated 3 minutes of time-series acquired acceleration into smaller non-overlapping 10-second windows, resulting in 18 windows ($\frac{3\times60}{10} = 18$). Furthermore, for the real-life experiment, we deployed only one event with duration of 15 seconds captured by all the sensors to avoid any heterogeneity in the frequency domain evaluation. Consider that a window size of more than 10 seconds does not impact the result of PSD since no structural response lasts for more than 10 seconds. However, windows of less than 5 seconds cause a drop in the accuracy of frequency analysis.

The first part of Tab. III reports the results obtained for the LAB experiments. The excitation stimuli applied by the shaker has a frequency of 10 Hz, which is captured as the first natural frequency by all the sensors in all scenarios. Notice that ISM in LP mode works as accurately as the piezoelectric sensor, even in the smallest input range. Compared to the piezoelectric sensor, the most accurate sensor, the results reported in the peak amplitude section of Tab. III indicate 11.5%, 4.0%, and 3.4% deviation for LIS, ISM in HP, and ISM in LP mode in peak frequencies' amplitude identification, respectively. Considering the width of the natural frequency, the last section of Tab. IV indicates a very narrow window for all the peak frequencies, fixed at 0.1 Hz for all the sensors. Furthermore, the second part of Tab. III reports the result of

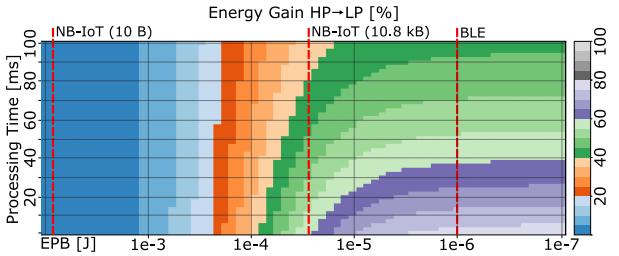

Fig. 2. Low-Power energy gain as a function of processing time and EPB.

the real-life event. Considering the peak frequency, the piezo sensor identifies 5.5 Hz, further characterised by the MEMS sensor. The peak amplitude section of Tab. III demonstrates that similar to the Lab experiment, the analog MEMS deviates the most by 1.86 μg, i.e., 34.5% compared to the piezo one. Notice that digital MEMS in the LP mode also reports 1.4 μg (25%) mismatch compared to the accurate piezo sensors and with dissimilarities close to analog one. This mismatch is due to the low sampling rate of both MEMS, where they cannot capture the whole amplitude of the exciting stimuli. Finally, the peak width section in Tab. III provides similar results to that of peak amplitude, in the sense that digital MEMS, ISM in HP mode, is capable of following piezo sensor, whereas analog and digital MEMS in LP mode deviates from piezo by 0.03 Hz. The former results mainly characterize two outcomes. The former is both analog and digital MEMS sensors are feasible candidates to replace the costly, power-hungry piezo sensors, whereas the latter is the fact that low sampling frequency can achieve reasonable accuracy modal frequency analysis and peak width up to maximun 7% error rates. Although deploying a lower sampling rate impacts parameters like network traffic, it performs less accurately than a high sampling rate one, given the peak amplitudes parameter.

D. Low-Power mode energy characterization

We evaluate Low-Power mode energy savings for the workload presented in Subsection VI-D. The MEMS measures for 10 s and the MCU runs a damage detection algorithm that summarises the health status of the structure in a 10 Bytes payload that is sent to the cloud. The processing time and the EPB required to send data remotely are considered free variables in our model. EPB is contained within the range $10^{-2} - 10^{-7}$ Joule that comprises two widely used transmission technologies, namely BLE [11] and NB-IoT [4]. We assume damage detection pipelines can summarize structure behaviour within 10 Bytes. Choosing sensor sampling time needs more care since a hidden relationship exists between the amount of data a application generates and its processing time. Such a exploration is left as a future work since it requires assumptions on the asymptotic complexity of the algorithm run on the MCU. Here, we focus on postprocessing algorithms able to process 10 s measurements data within 100 ms.

Table IV details the power and energy numbers used to feed the energy model. ISM330DHCX High-Performance and Low-Power consumption is characterized while reading accelerations at a rate of 104 Hz with the SPI peripheral driven at 8 MHz. The radio works in three modes along the four application stages. In stages a and b it is off, in stage c it

TABLE III
IN-FREQUENCY ANALYSIS FOR THE LAB AND BEAM EXPERIMENTS.

Experiment		Peak Frequency $[Hz]$				Peak Amplitude $[mg]$				Peak Width $[Hz]$			
		PCB	LIS	ISM_H	ISM_L	PCB	LIS	ISM_H	ISM_L	PCB	LIS	ISM_H	ISM_L
LAB	$30\,\mu m$	10	10	10	10	0.05	0.04	0.05	0.05	0.1	0.1	0.1	0.1
	$250\,\mu m$	10	10	10	10	4.80	4.23	4.50	4.03	0.1	0.1	0.1	0.1
Experiment		Peak Frequency $[Hz]$				Peak Amplitude $[\mu g]$				Peak Width $[Hz]$			
BEAM		5.5	5.5	5.5	5.5	5.39	3.53	5.60	6.79	0.4	0.4	0.4	0.4

TABLE IV
ENERGY MODEL PARAMETERS

Component	Status	Power [W]	Condition
MCU	Run	5.5e-2	Core clock at 80 MHz
	Idle	4.0e-6	SoC driven in STOP mode
MEMS	Off	3.0e-6	-
	HP	6.5e-4	f_s = 104 Hz, SPI_{bps} = 8 MHz
	LP	1.0e-4	
Radio	Off	0.0e+0	-
	Active	5.5e-2	Estimated
Component	Status	EPB $[\mu J]$	Condition
Radio	TX	8912	NB-IoT (10 B packet)
		43	NB-IoT (10 kB packet)
		1	Bluetooth Low Energy

is active but it does not transmit anything, while in stage d it is active and it sends data to the cloud. Modelling radio consumption in stage c is challenging because it depends on many factors such as silicon manifacturing technology, radio microcontroller internal clock speed and whether radio chip is embedded in the same SoC of the MCU or not. In this work, we model radio transceiver active state as an additional microcontroller and we assign the same power consumption of the MCU in run mode. The rationale behind this choice is that we assume radio in active state behaves as a low-power microcontroller that handles the chip I/O interfaces while keeping the antenna and the transceiver off.

Figure 2 shows the energy gain obtained using a Low-Power mode sensor in place of the High-Performance one for different processing times and EPB. The plot highlights the existence of two interesting regions corresponding to radios characterized by EPB larger than 10^{-3} and smaller than 10^{-5}. For expensive technologies, such as NB-IoT, energy gain is largely independent on processing time and lower than 5%. The reason is that any gain obtained by collecting data in Low-Power mode is neglected by the energy required for transmission. Notice that, according to the NB-IoT energy characterization provided by the authors of [4], larger payloads lower EPB to 43 μJ, which would increases energy gain up to 60 %. This is the case for applications where make sense to collect a number of results on the edge before sending data to the cloud. Cheap communication technologies, such as BLE, show a energy gain larger than 40 %, bounded by the processing time required to run the damage detection pipeline. In this scenario, the design knobs available to increase energy gain are either selecting a less intensive processing pipeline or to select a MCU able to deliver a larger amount of FLOPS per Joule consumed.

VII. CONCLUSIONS

In this work, we provide an experimental evaluation of analog and digital MEMS accelerometers for structural health monitoring applications. Low-Power mode, a configuration available for modern digital MEMS is also tested from the metrological and energy efficiency point of view. Initially, we discuss the three criteria by which sensors are evaluated: the time and frequency domain and the energy modelling domain. Noise analysis of the sensors shows that the piezoelectric sensor is the less noisy device, with only $10.28\mu g/\sqrt{(}Hz)$. While in-lab experiments show that MEMS low-cost sensors mimic piezo sensors for modal frequency analysis, we show in the real-life experiment that MEMS-based accelerations diverge maximum by 1.6% error. Finally, we quantify energy efficiency of Low-Power mode compared to High-Performance ones, for different transmission technologies. Energy gain stands between 40% and 80% for BLE, depending on the MCU processing time. Lastly, NB-IoT energy gain can reach up to 60% if larger payloads are considered, while it is 5% for 10 B of payload.

ACKNOWLEDGMENT

This work was supported by INSIST Project (PON Ricerca e Innovazione 2014-2020).

REFERENCES

[1] A. Sabato *et al.*, "Wireless mems-based accelerometer sensor boards for structural vibration monitoring: a review," *IEEE Sensors Journal*, 2016.

[2] R. R. Ribeiro *et al.*, "Evaluation of low-cost mems accelerometers for shm: Frequency and damping identification of civil structures," *Latin American Journal of Solids and Structures*, 2019.

[3] C. Bedon *et al.*, "Prototyping and validation of mems accelerometers for structural health monitoring—the case study of the pietratagliata cable-stayed bridge," *Journal of Sensor and Actuator Networks*, 2018.

[4] F. Di Nuzzo *et al.*, "Structural health monitoring system with narrow-band iot and mems sensors," *IEEE Sensors Journal*, 2021.

[5] A. D'Alessandro *et al.*, "A review of the capacitive mems for seismology," *Sensors*, 2019.

[6] A. Albarbar *et al.*, "Performance evaluation of mems accelerometers," *Measurement*, 2009.

[7] C. Acar *et al.*, "Experimental evaluation and comparative analysis of commercial variable-capacitance mems accelerometers," *Journal of micromechanics and microengineering*, 2003.

[8] S. Kavitha *et al.*, "High performance mems accelerometers for concrete shm applications and comparison with cots accelerometers," *Mechanical Systems and Signal Processing*, 2016.

[9] A. Sivasuriyan *et al.*, "Performance of rc beams utilizing various sensors under fundamental static loading," *International Journal of System Assurance Engineering and Management*, 2022.

[10] F. Barchi *et al.*, "Spiking neural network-based near-sensor computing for damage detection in structural health monitoring," *Future Internet*, 2021.

[11] S. Aguilar *et al.*, "Opportunistic sensor data collection with bluetooth low energy," *Sensors*, 2017.